Analysis of the Coverage of Tunable Matching Networks with Three Tunable Elements

Eyad Arabi, Xingran Jiao, Kevin Morris and Mark Beach
Communication Systems and Networks Research Group
Uniersity of Bristol
Bristol, BS8 1UB, UK
Email: {eyad.arabi, kevin.morris}@bristol.ac.uk

***Abstract*—Tunable matching networks are crucial for agile radio frequency circuits. To optimally design such networks the overall coverage needs to be determined. In this work, analytical formulas for the coverage area within the Smith chart of a three-element tunable-network are derived. It has been found that up to sixteen circles bound the coverage area. Analytical expressions for the centers and radii of these circles have been derived and verified by circuit simulation as well as measured data. The formulas in this work can be readily integrated into CAD tools, thus provide a valuable tool for the design of tunable circuits.**

I. Introduction

Reconfigurable wireless transceivers are becoming very important for future systems such as long term evolution (LTE) and LTE-advanced. At the heart of such systems, are tunable circuits like filters, antennas, and matching networks (MN). The latter are important to design power amplifiers [1] and antennas [3].

Lumped-based MNs are very attractive at frequencies below three GHz due to their small form factors and high qualities. Variable capacitors and inductors can be used to design tunable networks. Since variable inductors can not be physically realized, a variable capacitor in parallel with a fixed inductor can be used. A typical topology with three tunable elements is analyzed in this work as illustrated in Fig. 1.

One of the main characteristics the RF designer needs to know about a tunable MN is the range of complex impedances that it can match to a specific load (typically 50 Ohm). This range of impedances can be described by an area within the Smith chart. In [4], formulas for the coverage area have been derived for the rectangular complex-impedance plane. It is more useful to provide the coverage on the Smith chart because it can be presented against other design metrics [5]. In our previous work [6], we have derived analytical formulas for the coverage in the Smith chart for networks with two tunable elements. In this paper, analytical formulas for a matching network with three tunable elements (Fig. 1) are presented for the first time. It has been found that the boundary of the coverage area consists of up to sixteen arcs. Analytical formulas for the radii and centers of these arcs have been derived. These formulas are suitable for CAD tools and the same analysis method presented here can be used for networks with more or less tunable components. Therefore, this analysis provides a convenient tool to design and optimize tunable matching networks.

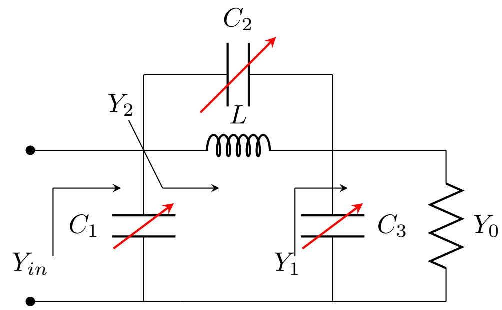

Fig. 1. Schematic of the tunable matching network analyzed in this work.

II. Derivation of the Boundary Circles

In [4] it was found that as one tunable parameter of the matching network is varied between its limits while all the others are kept constant, the locus of the matched impedance follows an arc on the impedance plane. Since the relation between the complex impedance plane and the Γ plane is a bilinear transformation, circles on the complex plane are mapped into circles on the Γ-plane [7]. Therefore, the coverage area of any matching network is bounded by circles in the Smith chart. If the centers and radii of these circles are calculated, the boundary can be defined. A typical boundary for the network of Fig. 1 is illustrated in Fig. 3-a & b.

Three main cases can be considered for the circuit of Fig. 1 by sweeping each of the tunable capacitors while keeping the other two at constant values (minimum (m) or maximum (x)). From each case four circles are obtained for the combinations of the maximum and minimum of the two constant capacitors (mm, mx, xm, and xx) resulting in a total of twelve circles. Moreover, if C_2, C_3, and L are in resonance, the coverage area might be extended by up to four additional circles, which are referred to here as *auxiliary* circles. All of the sixteen circles are tangential to the circle of $|\Gamma|$=1. If the tangent point is denoted A(x_A,y_A) and point B(x_B,y_B) is *any* other point, the center (x_c, y_c) and radius (R_c) can be calculated by:

$$x_c = \frac{x_A\left(x_B^2 - x_A^2 + y_B^2 - y_A^2\right)}{2\left(-x_A^2 - y_A^2 + x_A x_B + y_A y_B\right)}, \quad (1a)$$

$$y_c = \frac{y_A\left(x_B^2 - x_A^2 + y_B^2 - y_A^2\right)}{2\left(-x_A^2 - y_A^2 + x_A x_B + y_A y_B\right)} \quad \text{and} \quad (1b)$$

$$R_c = \sqrt{(x_c - x_A)^2 + (y_c - y_B)^2}, \quad (1c)$$

respectively. These equations are used in the following sections to define the circles of the boundary.

A. C_1 variable, C_2 and C_3 are fixed

In the first case C_2 and C_3 are fixed at either their minimum ($C_{i,min}$, i=2,3) or maximum ($C_{i,max}$, i=2,3) while C_1 is varied between its limits. For the sake of mathematical convenience, C_3 will be allowed to take negative as well as positive values. The tangent point can be found by assigning infinity to C_1, which results in a short at the input of the matching network; therefore, the coordinates of the reflection coefficient are given by:

$$x_{A1} = -1 \qquad \text{and} \tag{2a}$$

$$y_{A1} = 0. \tag{2b}$$

For the other point C_1 can be assigned a value of zero and the real and imaginary parts of the input admittance Y_{in} can be calculated as:

$$\Re\{Y_{in}\} = \frac{\left(\frac{1}{\omega L} - \omega C_2\right)\left[Y_0 \omega C_3 - Y_0\left(\omega\left(C_3 + C_2\right) - \frac{1}{\omega L}\right)\right]}{Y_0^2 + \left(\omega\left(C_3 + C_2\right) - \frac{1}{\omega L}\right)^2} \tag{3a}$$

and

$$\Im\{Y_{in}\} = \frac{\left(\omega C_2 - \frac{1}{\omega L}\right)\left[Y_0^2 + \omega C_3\left(\omega\left(C_3 + C_2\right) - \frac{1}{\omega L}\right)\right]}{Y_0^2 + \left(\omega\left(C_3 + C_2\right) - \frac{1}{\omega L}\right)^2}, \tag{3b}$$

from which the real and imaginary values of Γ_{in} are:

$$x_{B1} = \frac{-\left(\Re\{Y_{in}\}\right)^2 + Y_0^2 - \left(\Im\{Y_{in}\}\right)^2}{\left(\Re\{Y_{in}\} + Y_0\right)^2 + \left(\Im\{Y_{in}\}\right)^2} \quad \text{and} \tag{4a}$$

$$y_{B1} = \frac{-2Y_0 \Im\{Y_{in}\}}{\left(\Re\{Y_{in}\} + Y_0\right)^2 + \left(\Im\{Y_{in}\}\right)^2}, \tag{4b}$$

respectively. The results of (2), (3) and (4) can be used with (1) to calculate the circle parameters for this case.

B. C_2 variable, C_1 and C_3 are fixed

In this case C_1 and C_3 are fixed at either their minimum ($C_{i,min}$, i=1,3) or maximum ($C_{i,max}$, i=1,3) while C_2 is varied between its limits. The tangent point occurs when $C_2 = 1/(\omega^2 L)$ and its coordinates are given by

$$x_{A2} = \frac{Y_0^2 - \left(\omega C_3\right)^2}{Y_0^2 + \left(\omega C_3\right)^2} \tag{5a}$$

and

$$y_{A2} = \frac{-2Y_0 \omega C_3}{Y_0^2 + \left(\omega C_3\right)^2}. \tag{5b}$$

The second point is calculated by assigning infinity to C_2 and calculating the real and imaginary parts of Y_{in} as

$$\Re\{Y_{in}\} = 0 \quad \text{and} \tag{6a}$$

$$\Im\{Y_{in}\} = \omega\left(C_1 + C_3\right), \tag{6b}$$

respectively. Equations (5), (6) and (4) can be used with (1) to calculate the boundary circles for this case.

C. C_3 variable, C_1 and C_2 are fixed

In this case C_1 and C_2 are fixed at either their minimum ($C_{i,min}$, i=1,2) or maximum ($C_{i,max}$, i=1,2) while C_3 is varied between its limits. The tangent point occurs when C_3 is assigned a value of infinity to give real and imaginary values of Y_{in} as

$$\Re\{Y_{in}\} = 0 \quad \text{and} \tag{7a}$$

$$\Im\{Y_{in}\} = \omega\left(C_2 + C_1\right) + \frac{1}{\omega L}, \tag{7b}$$

respectively. The second point is calculated by assigning zero to C_3 and calculating the real and imaginary parts of Y_{in} as

$$\Re\{Y_{in}\} = \frac{Y_0\left(\omega C_2 - \frac{1}{\omega L}\right)^2}{Y_0^2 + \left(\omega C_2 - \frac{1}{\omega L}\right)^2} \quad \text{and} \tag{8a}$$

$$\Im\{Y_{in}\} = \omega C_1 + \frac{Y_0^2\left(\omega C_2 - \frac{1}{\omega L}\right)}{Y_0^2 + \left(\omega C_2 - \frac{1}{\omega L}\right)^2}, \tag{8b}$$

respectively. Equations (7) and (8) can be used with (4) to calculate the coordinates of the two points, which can be used with (1) to calculate the boundary circles.

D. The auxiliary circles

As discussed previously, up to four auxiliary circles might be part of the boundary. These circles result from a resonance condition of C_2, C_3 and L. Therefore, they define maximum and/or minimum input conductances and they do not depend on C_1. They can be plotted using the relations derived for variable C_1 in section II-A with *appropriate* values of C_2 and C_3 obtained by evaluating the maximum and minimum of the input conductance. For simplicity, the combination of C_2 and L can be considered as a variable inductor with inductance of $L/(1-\omega^2 LC_2)$. The first derivative technique can be used to obtain the condition for maximum/minimum criteria as:

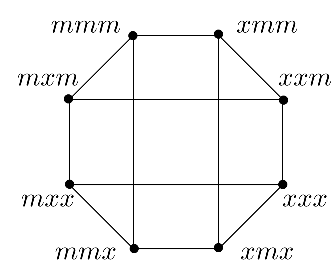

Fig. 2. Illustration of the twelve arcs of the boundary area. The two ends and any third point are sufficient to plot the arcs. The auxiliary arcs are not included.

$$C_2' + C_3' = \frac{1}{\omega^2 L}, \tag{9}$$

where C_2' and C_3' are the critical values of C_2 and C_3 at which resonance occurs. From this condition, up to four circles can be plotted by assigning the maximum and minimum capacitance to C_2' and evaluate C_3' from (9). Two circles can be plotted using these values with the variable C_1 circles derived previously. The other two circles can be plotted by reversing the assignment of C_2' and C_3'. If either of the evaluated values

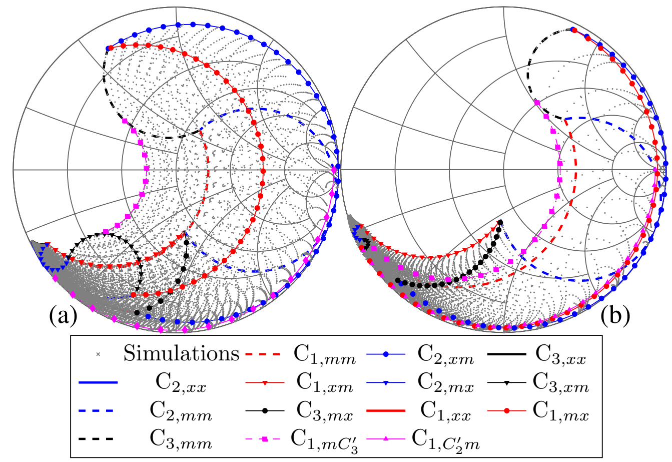

Fig. 3. Theoretical analysis and circuit simulation of the network of Fig. 1 at 2 GHz (a) and 3 GHz (b). Each arc is denoted by $C_{i,jk}$ to represent a variable C_i while the other two capacitors have constant values of j and k. $i \in \{1,2,3\}$, $j\&k \in \{m,x\}$, where m represents the minimum value and x represents the maximum value. The values used in the theory are: L=3nH, C_{min}=0.2 pF, and C_{max}=5 pF.

of C_2' and C_3' fall outside the range of C_{min}-C_{max}, the associated circle is not part of the boundary. Therefore, part or all of the auxiliary circles might not be necessary to define the boundary.

E. Connecting the Boundary Area

Formulas for the centers and radii of the sixteen different circles of the boundary have been derived in the previous sections. Many of these circles intersect at multiple points, therefore a systematic method to identify and connect the different arcs is described in this section. In Fig. 2 eight different points are presented for all the combinations of the maximum and minimum values of the three capacitors. These points are denoted ijk where i, j & $k \in \{m, x\}$ and m, x represent the minimum and maximum values, respectively. The boundary is defined by connecting these lines with twelve arcs each of which represent the variation of only one capacitor. To plot each arc the starting and ending points are first calculated from the constant values of the capacitors. Since the arcs can not be completely defined by their start and end points, a third point between these two points is also calculated. The arc can be plotted from these three points and the center and radius calculated in the previous section in a strait forward manner. If necessary, the auxiliary arcs can be plotted in a similar manner.

The calculated boundary is illustrated in Fig. 3 (a) and (b) for frequencies of 2 GHz and 3 GHz, respectively.

III. Measurement Results

A prototype has been fabricated and measured to verify the theoretical formulas derived in the previous section. A commercially available varactor (BB388 from Infineon) has been use as a variable capacitor. A photo of the fabricated prototype is shown in the inset of Fig. 4. The connectors and feed lines have been de-embedded and the final results are compared to the theory in Fig. 4. A good agreement between the simulation and measurement can be observed, which verifies the theoretical analysis. The discrepancies are mainly due to the package parasitics of the lumped components and de-embedding errors.

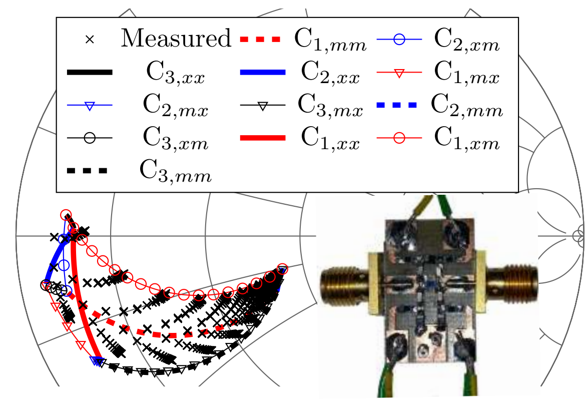

Fig. 4. Measured coverage area compared to the theory for a frequency of 1 GHz and with L=1.3 nH, C_{min}=1pF, and C_{max}= 10 pF. A photograph of the fabricated prototype is included in the inset.

IV. Conclusion

In this work, a method for the analysis of tunable matching networks is presented. Formulas for the coverage of a three-element matching network has been derived as proof of concept. It has been found that up to sixteen circles are needed to completely define the boundary area. The formulas are simple and can be used with CAD tools to analyze and optimize tunable matching networks.

Acknowledgment

This work is supported by the British Engineering and Physical Sciences Research Council (EPSRC), under the FARAD project with grant number EP/M01360X/1 in collaboration with the University of Sheffield.

References

[1] H. M. Nemati, C. Fager, U. Gustavsson, R. Jos, and H. Zirath, "Design of Varactor-Based Tunable Matching Networks for Dynamic Load Modulation of High Power Amplifiers," *IEEE Transactions on Microwave Theory and Techniques*, vol. 57, pp. 1110–1118, May 2009.

[2] D. Ji, J. Jeon, and J. Kim, "A Novel Load Mismatch Detection and Correction Technique for 3G/4G Load Insensitive Power Amplifier Application," *IEEE Transactions on Microwave Theory and Techniques*, vol. 63, pp. 1530–1543, May 2015.

[3] H. Y. Li, C. T. Yeh, J. J. Huang, C. W. Chang, C. T. Yu, and J. S. Fu, "CPW-Fed Frequency-Reconfigurable Slot-Loop Antenna With a Tunable Matching Network Based on Ferroelectric Varactors," *IEEE Antennas and Wireless Propagation Letters*, vol. 14, pp. 614–617, 2015.

[4] M. Thompson and J. K. Fidler, "Determination of the impedance matching domain of impedance matching networks," *IEEE Transactions on Circuits and Systems I: Regular Papers*, vol. 51, pp. 2098–2106, Oct 2004.

[5] T. Lee, "The Smith Chart Comes Home [President's Column]," *IEEE Microwave Magazine*, vol. 16, pp. 10–25, Nov 2015.

[6] E. Arabi, K. A. Morris, and M. Beach, "Analytical Formulas for the Coverage of Tunable Matching Networks for Reconfigurable Applications," *IEEE Transactions on Microwave Theory and Techniques*, Accepted, 2017.

[7] K. Miller, *Advanced Complex Calculus*. Harper's mathematics series, Harper, 1960.